

Brain Tumor Segmentation Based on SFCM using Back Propagation Neural Network

Y Aruna

Assistant Professor,
Department of ECE

Vidya Jyothi Institute of Technology.

M Madhavi

M.Tech Student,
Department of ECE

Vidya Jyothi Institute of Technology.

Abstract:

Automatic defects detection in MR images is very important in many diagnostic and therapeutic applications. Because of high quantity data in MR images and blurred boundaries, tumour segmentation and classification is very hard. This work has introduced one automatic brain tumour detection method to increase the accuracy and yield and decrease the diagnosis time. The goal is classifying the tissues to three classes of normal, benign and malignant. In MR images, the amount of data is too much for manual interpretation and analysis. During past few years, brain tumor segmentation in magnetic resonance imaging (MRI) has become an emergent research area in the field of medical imaging system. Accurate detection of size and location of brain tumor plays a vital role in the diagnosis of tumor. The diagnosis method consists of four stages, pre-processing of MR images, feature extraction, and classification. After histogram equalization of image, the features are extracted based on Dual-Tree Complex wavelet transformation (DTCWT).

In the last stage, Back Propagation Neural Network (BPN) are employed to classify the Normal and abnormal brain. An efficient algorithm is proposed for tumor detection based on the Spatial Fuzzy C-Means Clustering.

Index Terms—Magnetic Resonance Imaging, Glioma, Brain Tumor, Brain Tumor Segmentation, back propagation neural network classifier, Dual-Tree Complex wavelet transformation(dtcwt), Spatial Fuzzy C-Means Clustering(SFCM), Gray level co occurrence matrix(GLCM).

I INTRODUCTION

Gliomas are the brain tumors with the highest mortality rate and prevalence. These neoplasms can be graded into Low Grade Gliomas (LGG) and High Grade Gliomas (HGG), with the former being less aggressive and infiltrative than the latter. Even under treatment, patients do not survive on average more than 14 months after diagnosis. Current treatments include surgery, chemotherapy, radiotherapy, or a combination of them. MRI is especially useful to assess gliomas in clinical practice, since it is possible to acquire MRI sequences providing complementary information. The accurate segmentation of gliomas and its intra-tumoral structures is important not only for treatment planning, but also for follow-up evaluations. However, manual segmentation is time-consuming and subjected to inter- and intra-rater errors difficult to characterize. Thus, physicians usually use rough measures for evaluation. For these reasons, accurate semi-automatic or automatic methods are required. However, it is a challenging task, since the shape, structure, and location of these abnormalities are highly variable. Additionally, the tumor mass effect change the arrangement of the surrounding normal tissues. Also, MRI images may present some problems, such as intensity in homogeneity, or different intensity ranges among the same sequences and acquisition scanners. In brain tumor segmentation, we find several methods that explicitly develop a parametric or non-parametric probabilistic model for the underlying data. These models usually include a likelihood function corresponding to the observations and a prior model. Being abnormalities, tumors can be segmented as outliers of normal tissue, subjected to shape and connectivity constrains. Other approaches rely on probabilistic atlases. In the case of brain tumors, the atlas

must be estimated at segmentation time, because of the variable shape and location of the neoplasms. Tumor growth models can be used as estimates of its mass effect, being useful to improve the atlases. The neighborhood of the voxels provides useful information for achieving smoother segmentations through Markov Random Fields (MRF). Zhao et al. also used a MRF to segment brain tumors after a first oversegmentation of the image into supervoxels, with a histogram-based estimation of the likelihood function. As observed by Menze et al., generative models generalize well in unseen data, but it may be difficult to explicitly translate prior knowledge into an appropriate probabilistic model. Another class of methods learns a distribution directly from the data. Although a training stage can be a disadvantage, these methods can learn brain tumor patterns that do not follow a specific model. This kind of approaches commonly consider voxels as independent and identically distributed, although context information may be introduced through the features. Because of this, some isolated voxels or small clusters may be mistakenly classified with the wrong class, some-times in physiological and anatomically unlikely locations. To overcome this problem, some authors include information of the neighborhood by embedding the probabilistic predictions of the classifier into a Conditional Random Field. Classifiers such as Support Vector Machines and, more recently, Random Forests (RF) were successfully applied in brain tumor segmentation. The RF became very used due to its natural capability in handling multi-class problems and large feature vectors. A variety of features were proposed in the literature: encoding context, first-order and fractals-based texture [gradients [brain symmetry [and physical properties. Using supervised classifiers, some authors developed other ways of applying them. Tustison et al. developed a two-stage segmentation framework based on RFs, using the output of the first classifier to improve a second stage of segmentation. Geremia et al. proposed a Spatially Adaptive RF for hierarchical segmentation, going from coarser to finer scales. Meier et al. used a semi-supervised RF to train a subject-specific classifier for post-operative brain tumor

segmentation. Other methods known as Deep Learning deal with representation learning by automatically learning an hierarchy of increasingly complex features directly from data. So, the focus is on designing architectures instead of developing hand-crafted features, which may require specialized knowledge. CNNs have been used to win several object recognition and biological image segmentation challenges. Since a CNN operates over patches using kernels, it has the advantages of taking context into account and being used with raw data. In the field of brain tumor segmentation, recent proposals also investigate the use of CNNs. Zikic et al. used a shallow CNN with two convolutional layers separated by max-pooling with stride 3, followed by one fully-connected (FC) layer and a softmax layer. In addition to their two-pathway network, Havaei et al. built a cascade of two networks and performed a two-stage training, by training with balanced classes and then refining it with proportions near the originals. Lyksborg et al. use a binary CNN to identify the complete tumor. Then, a cellular automata smooths the segmentation, before a multi-class CNN discriminates the sub-regions of tumor. Rao et al. extracted patches in each plane of each voxel and trained a CNN in each MRI sequence; the outputs of the last FC layer with softmax of each CNN are concatenated and used to train a RF classifier. Dvořák and Menze [35] divided the brain tumor regions segmentation tasks into binary sub-tasks and proposed structured predictions using a CNN as learning method. Patches of labels are clustered into a dictionary of label patches, and the CNN must predict the membership of the input to each of the clusters. In this paper, inspired by the groundbreaking work of Simonyan and Zisserman on deep CNNs, we investigate the potential of using deep architectures with small convolutional kernels for segmentation of gliomas in MRI images. Simonyan and Zisserman proposed the use of small 3×3 kernels to obtain deeper CNNs. With smaller kernels we can stack more convolutional layers, while having the same receptive field of bigger kernels. For instance, two 3×3 cascaded convolutional layers have the same effective receptive field of one 5×5 layer, but fewer weights. At the same time, it has the advantages

of applying more nonlinearities and being less prone to overfitting because small kernels have fewer weights than bigger kernels. We also investigate the use of the intensity normalization method proposed by Nyul et al. as a pre-processing step that aims to address data heterogeneity caused by multi-site multi-scanner acquisitions of MRI images. The large spatial and structural variability in brain tumors are also an important concern that we study using two kinds of data augmentation. The remainder of this paper is organized as follows. In Section II, the proposed method is presented. The databases used for evaluation and the experimental setup are detailed in Section III. Results are presented and discussed in Section IV. Finally, the main conclusions are presented in Section V.

II. PROPOSED METHOD

Fig. 1 presents an overview of the proposed approach. There are four main stages: pre-processing, feature extraction through Gray level co-occurrence matrix (GLCM), classification via Back propagation neural network (BPN) and post-processing.

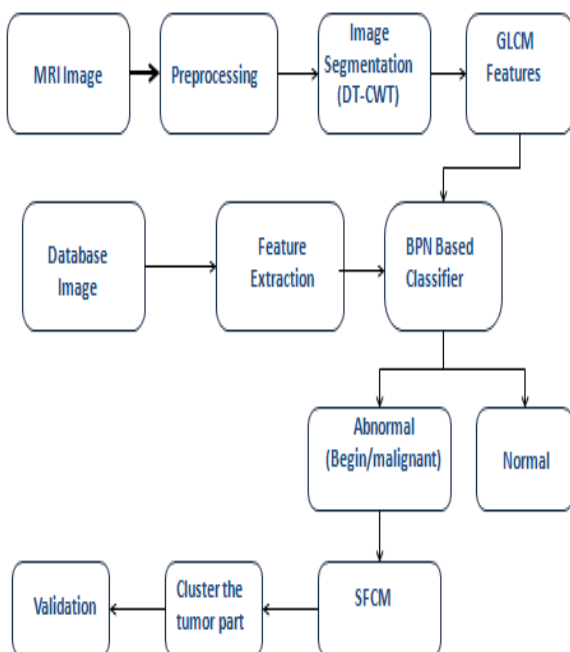


Fig. : Overview of the proposed method.

Pre-processing:

MRI images are altered by the bias field distortion. This makes the intensity of the same tissues to vary across the image. To correct it, we applied the N4ITK method [6].

However, this is not enough to ensure that the intensity distribution of a tissue type is in a similar intensity scale across different subjects for the same MRI sequence, which is an explicit or implicit assumption in most segmentation methods [37]. In fact, it can vary even if the image of the same patient is acquired in the same scanner in different time points, or in the presence of a pathology [7], [38]. So, to make the contrast and intensity ranges more similar across patients and acquisitions, we apply the intensity normalization method proposed by Nyul et al. on each sequence. In this intensity normalization method, a set of intensity landmarks $I_L = \{p_{c1}; i_{p10}; i_{p20}; i_{p90}; p_{c2}\}$ are learned for each sequence from the training set. p_{c1} and p_{c2} are chosen for each MRI sequence as described. i_{p1} represents the intensity at the 1th percentile. After training, the intensity normalization is accomplished by linearly transforming the original intensities between two landmarks into the corresponding learned landmarks. In this way, the histogram of each sequence is more similar across subjects. After normalizing the MRI images, we compute the mean intensity value and standard deviation across all training patches extracted for each sequence. Then, we normalize the patches on each sequence to have zero mean and unit variance¹. The mean and standard deviation computed in the training patches are used to normalize the testing patches.

Feature extraction through GLCM:

Feature extraction is the procedure of data reduction to find a subset of helpful variables based on the image. In this work, seven textural features based on the gray level co-occurrence matrix (GLCM) are extracted from each image. Co-occurrence matrices are calculated for four directions: 0°, 45°, 90° and 135° degrees. The seven Haralick texture descriptors are extracted from each co-occurrence matrices which are computed in each of four angles. Energy, Contrast, Homogeneity, correlation

$$\text{Energy} : \sum_{i,j} P(i, j)^2$$

$$\text{Homogeneity} : \sum_{i,j} \frac{1}{1+(i-j)^2} P(i, j)$$

$$\text{Correlation} : - \sum_{i,j} \frac{(i-\mu)(j-\mu)}{\sigma^2} P(i, j)$$

$$\text{Contrast} : \sum_{i,j} |i-j|^2 P(i, j)$$

Back propagation neural network (BPN):

Multilayer neural networks use a most common technique from a variety of learning technique, called the back propagation algorithm. In back propagation neural network, the output values are compared with the correct answer to compute the value of some predefined error function. By various techniques the error is then fed back through the network. Using this information, the algorithms adjust the weights of each connection in order to reduce the value of the error function by some small amount. After repeating this process for a sufficiently large number of training cycles the network will usually converge to some state where the error of the calculation is small.

The optimization algorithm repeats a two phase cycle, propagation and weight update. When an input vector is presented to the network, it is propagated forward through the network, layer by layer, until it reaches the output layer. The output of the network is then compared to the desired output, using a loss function, and an error value is calculated for each of the neurons in the output layer. The error values are then propagated backwards, starting from the output, until each neuron has an associated error value which roughly represents its contribution to the original output

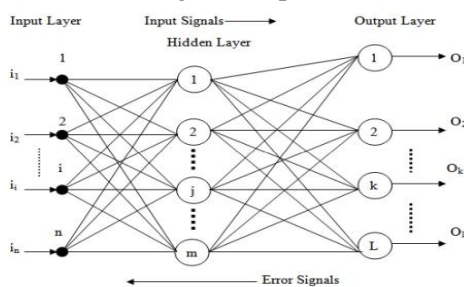
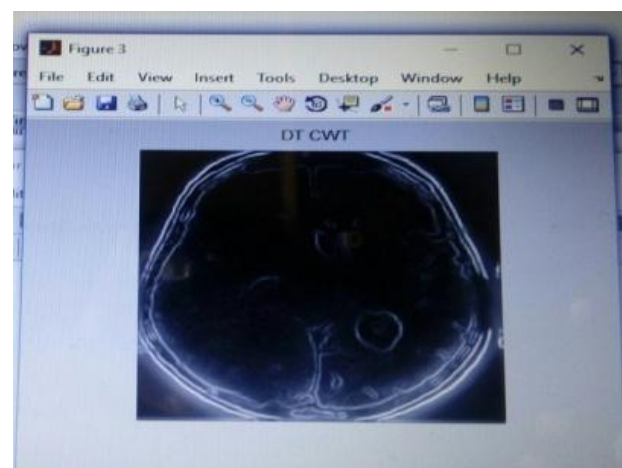
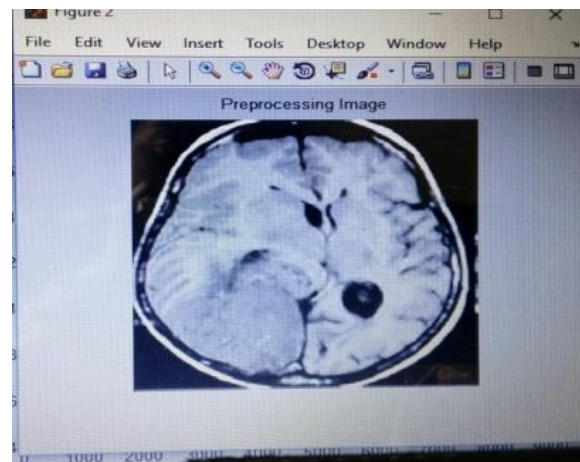
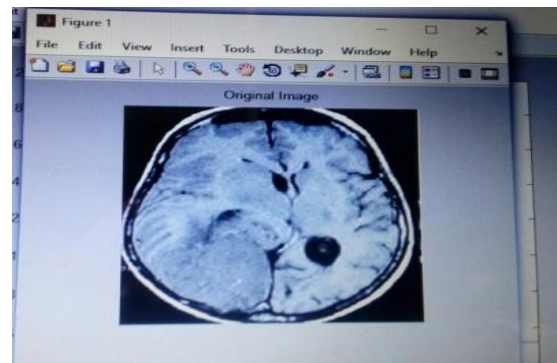


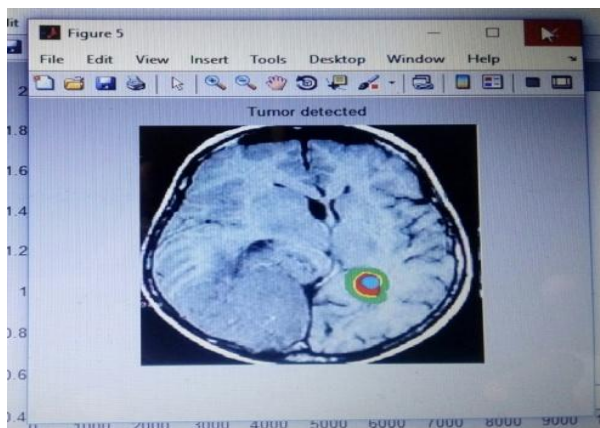
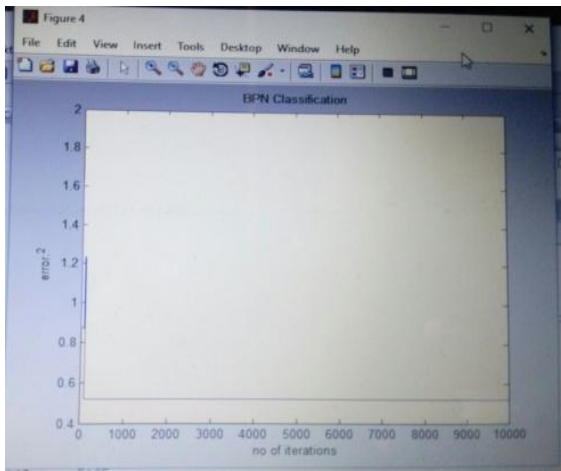
Figure Three layer back-propagation neural network

Post-processing:

Some small clusters may be erroneously classified as tumor. To deal with that, we impose volumetric constrains by removing clusters in the segmentation obtained by the CNN that are smaller than a predefined threshold t_{VOL} .

III. RESULTS





IV. CONCLUSION

In summary, we propose a novel CNN-based method for segmentation of brain tumors in MRI images. We start by a pre-processing stage consisting of bias field correction, intensity and patch normalization. After that, during training, the number of training patches is artificially augmented by rotating the training patches, and using samples of HGG to augment the number of rare LGG classes. The CNN is built over convolutional layers with small 3 3 kernels to allow deeper architectures. In designing our method, we address the heterogeneity caused by multi-site multi-scanner acquisitions of MRI images using intensity normalization as proposed by Nyul et al. We show that this is important in achieving a good segmentation. Brain tumors are highly variable in their spatial localization and structural composition, so we have investigated the use of data augmentation to cope with such variability.

We studied augmenting our training data set by rotating the patches as well as by sampling from classes of HGG that were underrepresented in LGG. We found that data augmentation was also quite effective, although not thoroughly explored in Deep Learning methods for brain tumor segmentation. Also, we investigated the potential of deep architectures through small kernels by comparing our deep CNN with shallow architectures with larger filters. We found that shallow architectures presented a lower performance, even when using a larger number of feature maps. Finally, we verified that the activation function LReLU was more important than ReLU in effectively training our CNN. We evaluated the proposed method in BRATS 2013 and 2015 databases.

Concerning 2013 database, we were ranked in the first position by the online evaluation platform. Also, it was obtained simultaneously the first position in DSC metric in the complete, core, and enhancing regions in the Challenge data set. Comparing with the best generative model, we were able to reduce the computation time approximately by ten-fold. Concerning the 2015 database, we obtained the second position among twelve contenders in the on-site challenge. We argue, therefore, that the components that were studied have potential to be incorporated in CNN-based methods and that as a whole our method is a strong candidate for brain tumor segmentation using MRI images.

REFERENCES:

- [1] S. Bauer et al., "A survey of mri-based medical image analysis for brain tumor studies," *Physics in medicine and biology*, vol. 58, no. 13, pp. 97–129, 2013.
- [2] D. N. Louis et al., "The 2007 WHO classification of tumours of the central nervous system," *Acta neuropathologica*, vol. 114, no. 2, pp. 97–109, 2007.
- [3] E. G. Van Meir et al., "Exciting new advances in neuro-oncology: The avenue to a cure for malignant glioma," *CA: a cancer journal for clinicians*, vol. 60, no. 3, pp. 166–193, 2010.

- [4] G. Tabatabai et al., "Molecular diagnostics of gliomas: the clinical perspective," *Acta neuropathologica*, vol. 120, no. 5, pp. 585–592, 2010.
- [5] B. Menze et al., "The multimodal brain tumor image segmentation benchmark (brats)," *IEEE Transactions on Medical Imaging*, vol. 34, no. 10, pp. 1993–2024, 2015.
- [6] N. J. Tustison et al., "N4itk: improved n3 bias correction," *IEEE Transactions on Medical Imaging*, vol. 29, no. 6, pp. 1310–1320, 2010. L. G. Nyul, J. K. Udupa, and X. Zhang, "New variants of a method of mri scale standardization," *IEEE Transactions on Medical Imaging*, vol. 19, no. 2, pp. 143–150, 2000.
- [7] Pham, D. L., 2003. Unsupervised tissue classification in medical images using edge-adaptive clustering. *Proceedings of the 25th Annual International Conference of the IEEE Engineering in Medicine and Biology Society*, Sep. 17-21, IEEE Xplore Press, pp: 634-637.
- [8] Christ, M. C. J. Parvathi, R. M. S. 2011 Fuzzy c-means algorithm for medical image segmentation *Electronics Computer Technology (ICECT)*.
- [9] B. H. Menze et al., "A generative model for brain tumor segmentation in multi-modal images," in *Medical Image Computing and Computer-Assisted Intervention–MICCAI 2010*. Springer, 2010, pp. 151–159.
- [10] A. Gooya et al., "Glistr: glioma image segmentation and registration," *IEEE Transactions on Medical Imaging*, vol. 31, no. 10, pp. 1941–1954, 2012.
- [11] D. Kwon et al., "Combining generative models for multifocal glioma segmentation and registration," in *Medical Image Computing and Computer-Assisted Intervention–MICCAI 2014*. Springer, 2014, pp. 763–770.
- [12] S. Bauer, L.-P. Nolte, and M. Reyes, "Fully automatic segmentation of brain tumor images using support vector machine classification in combination with hierarchical conditional random field regularization," in *Medical Image Computing and Computer-Assisted Intervention–MICCAI 2011*. Springer, 2011, pp. 354–361.
- [13] C.-H. Lee et al., "Segmenting brain tumors using pseudo-conditional random fields," in *Medical Image Computing and Computer-Assisted Intervention–MICCAI 2008*. Springer, 2008, pp. 359–366.
- [14] R. Meier et al., "A hybrid model for multimodal brain tumor segmentation," in *Proceedings of NCI-MICCAI BRATS, 2013*, pp. 31–37.
- [15] "Appearance-and context-sensitive features for brain tumor segmentation," in *MICCAI Brain Tumor Segmentation Challenge (BraTS), 2014*, pp. 20–26.
- [16] D. Zikic et al., "Decision forests for tissue-specific segmentation of high-grade gliomas in multi-channel mr," in *Medical Image Computing and Computer-Assisted Intervention–MICCAI 2012*. Springer, 2012, pp. 369–376.
- [17] S. Bauer et al., "Segmentation of brain tumor images based on integrated hierarchical classification and regularization," *Proceedings of MICCAI BRATS*, pp. 10–13, 2012.
- [18] S. Reza and K. Iftekharuddin, "Multi-fractal texture features for brain tumor and edema segmentation," in *SPIE Medical Imaging. International Society for Optics and Photonics, 2014*, pp. 903 503–903 503.
- [19] N. Tustison et al., "Optimal symmetric multimodal templates and concatenated random forests for supervised brain tumor segmentation (simplified) with antsr," *Neuroinformatics*, vol. 13, no. 2, pp. 209–225, 2015.
- [20] E. Geremia, B. H. Menze, and N. Ayache, "Spatially adaptive random forests," in *2013 IEEE 10th*



International Symposium on Biomedical Imaging (ISBI).
IEEE, 2013, pp. 1344–1347.

[21] A. Pinto et al., “Brain tumour segmentation based on extremely randomized forest with high-level features,” in Engineering in Medicine and Biology Society (EMBC), 2015 37th Annual International Conference of the IEEE. IEEE, 2015, pp. 3037–3040.

[22] A. Islam, S. Reza, and K. M. Iftekharuddin, “Multifractal texture estimation for detection and segmentation of brain tumors,” IEEE Transactions on Biomedical Engineering, vol. 60, no. 11, pp. 3204–3215, 2013.

[23] R. Meier et al., “Patient-specific semi-supervised learning for postoperative brain tumor segmentation,” in Medical Image Computing and Computer-Assisted Intervention–MICCAI 2014. Springer, 2014, pp.714–721.